International Journal of Thermophysics, Vol. 27, No. 6, November 2006 (© 2006)
DOI: 10.1007/s10765-006-0115-5

Transversely Oscillating MEMS Viscometer: The "Spider"[1]

K. A. Ronaldson,[2] A. D. Fitt,[2,3] A. R. H. Goodwin,[4] and W. A. Wakeham[5]

The analysis of a new viscometer that takes the form of an oscillating plate, fabricated from silicon using the methods of micro-electro-mechanical-systems (MEMS) is considered. The instrument is designed principally for experimental use in the oil industry. The plate is 1.6 mm wide, 2.4 mm long, and 20μm thick. It is suspended from a 0.4 mm thick support by 48 square cross-section legs, each of length 0.5 mm width and depth of 20μm. The process of lithography is used to deposit layers atop the silicon. These layers can then be formed into resistors and metallic tracks. The tracks traverse the supporting legs to provide connections between the plate and external electronics. The oscillating plate is a mechanical element that can be set in motion by the force produced by the interaction between an electric current flowing in the plate and an externally applied magnetic field. The viscometer can be operated either in forced or transient mode and is intended for use in both Newtonian and non-Newtonian fluids. The motion of the viscometer is analyzed for incompressible fluids, using the Navier–Stokes equations to model the flow for both a Newtonian viscous fluid and a viscoelastic fluid where the stress is modeled by a reduced form of Maxwell's equations.

KEY WORDS: down-hole; MEMS; non-Newtonian flow; viscometer.

[1] Paper presented at the Seventeenth European Conference on Thermophysical Properties, September 5–8, 2005, Bratislava, Slovak Republic.

[2] School of Mathematics, University of Southampton, Southampton SO17 1BJ, United Kingdom.

[3] To whom correspondence should be addressed. E-mail: adf@maths.soton.ac.uk

[4] Schlumberger Technology Corporation, 125 Industrial Blvd., Sugar Land, TX 77478, U.S.A.

[5] School of Engineering Sciences, University of Southampton, Southampton SO17 1BJ, United Kingdom.

1. INTRODUCTION

In this paper, we describe a transversely oscillating micro-electro-mechanical system (MEMS) device intended for use with down-hole fluids such as crude oil or brine. Viscometers are required to measure the thermophysical properties of fluids *in situ*, to determine optimal production strategies, and to exploit the value of the fluids in the well. In the oil exploration industry, the fluid viscosity can indicate the permeability of the reservoir formation, its flow characteristics, and the commercial value of the reservoir fluid. Currently, samples are collected from the reservoir and then later analyzed at the surface in a laboratory. The fluid properties and composition of a reservoir will change during its lifetime making it hard to simulate reservoir conditions in a laboratory. A hydrocarbon reservoir can exhibit temperatures of 20–200°C and pressures of 5–200 MPa. These conditions can be recreated in a laboratory but it is harder to replicate other effects such as fluid contamination and solid deposition. The rheology of the reservoir fluid is often measured at ambient conditions and then extrapolated to reservoir conditions. This requires a good model for the temperature and pressure dependence.

Conventional viscometers are currently unsuitable for *in situ* measurements for a host of reasons. Falling body viscometers contain free moving parts with small clearances between them that might be blocked by solids, such as sand, and prevent the body falling. Indeed, the orientation of the instrument with respect to the gravitational field must be known and this is not always the case. Capillary viscometers need not only a device to produce a constant fluid flow and measure the pressure drop but also an external pressure to balance the internal pressure so that distortions cannot occur in the tube. Torsional oscillating-body viscometers containing fluid can perform poorly at high pressures since it is inevitable that distortions in the dimensions of the body will occur. The damping effect on the discs of disc viscometers induced by liquids at such conditions is often so large that the mass of the disc required cannot be supported by any available method. The simple and compact vibrating wire viscometer is more appropriate for the far-from-ambient conditions that are found down-hole. It is able to work in hostile conditions because the wire body is electrically insulated from the pressure vessel [1]. Unfortunately, the use of the vibrating wire viscometer is limited by the equations used to evaluate the parameters in its mathematical model. By applying the Navier–Stokes equations, the model is only representative if the fluid tested is Newtonian. However, if the velocity of the wire is estimated for a range of currents and for several resonance frequencies it is plausible that vibrating wire viscom-

eters may provide useful information for non-Newtonian fluids. This concept has yet to be proven with measurements.

Clearly changes are needed to both the mechanical designs of the viscometers and the mathematical equations supporting them that are needed to interpret the measured quantities to provide precise values of the fluid viscosity in oil/gas wells *in situ*. This prompts the development of a new viscometer that will not only remain sufficiently accurate in hostile conditions but is also capable of measuring both Newtonian and non-Newtonian fluid properties. We recognize that a trade-off may have to be made between precision of the measurement and the ability to withstand hostile conditions as well as to operate within a wide range of fluids. The viscometer analyzed in this study enjoys a number of distinct advantages over alternative devices that are used in both Newtonian and non-Newtonian fluids: first, it contains only one moving part (all other components being electrical). Second, it is a factor of about 10 smaller and can therefore be mounted in confined spaces. Third, it requires no specific orientation with respect to the gravitational field. Finally, it can operate at pressures well in excess of ambient. We conclude that the production of a novel type of small-scale viscometer that can be used down-hole would be advantageous in this field.

Viscosity describes the internal friction of a moving fluid and its adhesive/cohesive or frictional properties. Fluids are termed "Newtonian" if they obey Newton's law of viscosity. Such fluids have a constant viscosity and density at a constant temperature and pressure whatever the shear rate. The Navier–Stokes equations for the motion of an incompressible Newtonian fluid [2] are:

$$\mathbf{q_t} + (\mathbf{q} \cdot \nabla)\mathbf{q} = -\frac{1}{\rho}\nabla p + \nu\nabla^2\mathbf{q} \tag{1}$$

$$\nabla \cdot \mathbf{q} = 0 \tag{2}$$

where $\mathbf{q}$ denotes the fluid velocity, p is the pressure, t is time, ρ is the fluid density, and ν is the kinematic viscosity.

Non-Newtonian fluids have a variable viscosity at a constant temperature and pressure that depends on the rate of shear and hence is referred to as a "shear-rate dependent" viscosity. Most fluids of this sort can be divided into one of the following three categories; a viscous fluid, an elastic fluid, or a viscoelastic fluid. In a purely viscous fluid all energy added is ultimately dissipated into temperature increase, whereas in a completely elastic fluid all the energy added is stored in the fluid and stress is directly proportional to strain. We can measure density in an incompressible non-Newtonian fluid but we have no analogous equation for the shear stress.

The viscosity may no longer be assumed to be constant and the shear stress must also be measured. In contrast to a Newtonian fluid, experiments yield a number of material functions that can depend on time, frequency, shear rate, and a host of other variables.

When testing is carried out during drilling for oil, it must be recognized that some drilling fluid additives are non-Newtonian. One such example is sodium bentonite, which is often added to increase the density of drilling mud. The properties of such muds can change after interaction with oil, formation rock or water, so that they exhibit different rheology. One such behavior is to reach a yield stress, then pass into a Bingham phase. Alternatively, a Hershel–Bulkley law is often an adequate description [3]. Schlumberger have carried out rheological tests on a number of water-based muds, such as may be present in an oil reservoir, at temperatures up to 130°C and pressures up to 100 MPa. From these results it has been deduced that muds have a largely pressure-independent yield stress with a sensitivity to temperature that increases with increasing temperature. As well as possessing a yield stress, such muds exhibit shear thinning behavior. It was found that this behavior could best be represented by a Herschel–Bulkley model.

The Herschel–Bulkley model employs a general law for viscosity that may be used to model non-Newtonian characteristics. Its formulation is

$$\tau = \tau_y + K\gamma^n \tag{3}$$

where τ is the stress, τ_y is the yield stress, γ is the shear rate, and K and n are constants. In the special case when $n=1$ and $\tau_y=0$, the fluid is Newtonian and K becomes the Newtonian viscosity μ.

In this study, we assume that the fluid is a homogeneous liquid. In both Newtonian and non-Newtonian cases, we assume that the fluid is incompressible and consider only harmonic non-Newtonian fluid motion.

2. SENSOR

The bulk of the sensor is made of anisotropic single crystal silicon with crystalline direction ⟨100⟩. We therefore assume that the mass and mechanical properties of the device will correspond those of pure silicon. To simplify the model, the silicon is assumed to be isotropic. The material properties in certain crystalline directions can be calculated from basic crystal properties. For silicon in the ⟨100⟩ plane, the isotropic values that best reflect the anisotropic behavior are given by Spiering et al. [4] and Petersen [5]. The MEMS fabrication process for the viscometer described in this study is, to all intents and purposes, the same as that described in

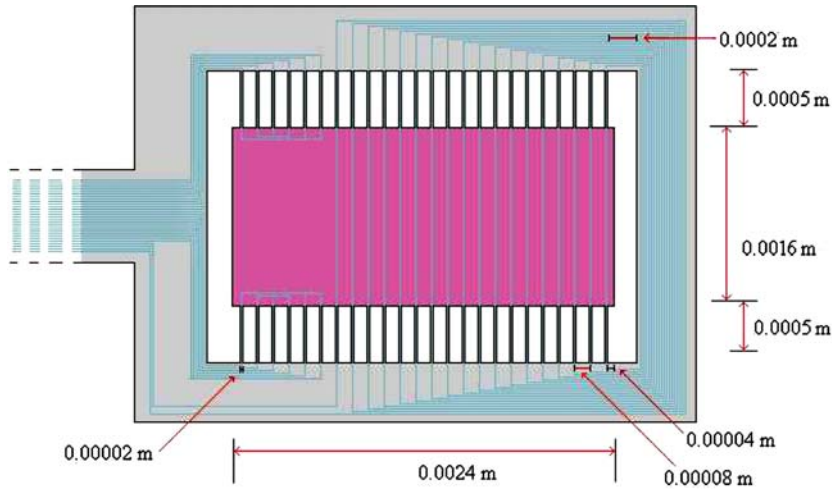

Fig. 1. Transversely oscillating MEMS.

Goodwin et al. [6] for an edge-clamped plate used to measure density and viscosity for Newtonian fluids.

The vibrating viscometer design described here is a MEMS (micro-electro-mechanical-system). The dimensions of the sensor are extremely small, its thickness and amplitude of motion being measured in μm. Exact dimensions are shown in Fig. 1. The device has both electrical and mechanical components. The oscillating plate is a mechanical element that can be set in motion when an alternating electric current I is passed through an aluminum wire coil atop the plate, which is held in an externally applied magnetic field. An external electromagnet or a fixed permanent magnet holds the plate in a constant magnetic field, B. This produces corresponding alternating forces, F, that force the plate to oscillate. This force can be altered by changing either the current or the intensity of the magnetic field. When the frequency of the current reaches the first natural frequency of the sensor, the plate will oscillate at the maximum amplitude in the first bending mode at its resonant frequency. These modes differ for each MEMS design.

The conductor and magnetic field that together make up the actuator have no interaction with the detector. The detectors used in this MEMS device and that of [6] are polysilicon piezoresistive strain gauges. These are placed at points where maximum and minimum strains occur and form a Wheatstone bridge. The optimum positioning was found using finite element analysis. This was carried out at Schlumberger Research using the finite element package ANSYS. The Wheatstone bridge is formed from the top six legs on each side, closed by wire-bonding. There are 24 legs on each

side. The gauges detect the varying strains in the sensor as it vibrates and enable one to measure a resonance frequency f and an associated quality factor Q. The resonance characteristics f and Q of the MEMS device will be affected by the addition of a surrounding fluid. Near to the surface of the vibrating sensor the fluid is moved, causing the addition of effective mass or inertia to the intrinsic mass of the plate. This results in a decrease in f. Q also decreases from the Q measured for a less viscous fluid since viscous energy is lost to the shearing motion of the fluid around the sides of the plate. Therefore, measurements of f and Q for a sensor in a fluid should allow the viscosity ν and density ρ of the fluid to be obtained.

3. MODELING THE DEVICE

We model the plate as an elastic solid that oscillates transversely in a fluid. Two different modes of operation for the determination of viscosity will be discussed. The "forced" mode is time-periodic, with the plate oscillating at a fixed forced frequency. We will also analyze the "plucked" problem, considering the transient or time-dependent behavior, where the amplitude of oscillation varies in time after an initial perturbation. We will consider the general case of incompressible fluids, using the Navier–Stokes equation to model Newtonian fluid motion and a reduced form of Maxwell's equations for viscoelastic fluid motion. One of the key aims of this study is to determine whether the device should be used in forced or plucked mode, and to identify the key physical parameters that may be used to optimize its operation.

The plate will oscillate at the maximum amplitude in the first bending mode at resonant frequency when the current reaches the first natural frequency of the sensor. An armature will generally possess several modes of vibration and thus give a complex interaction with the surrounding fluid. To obtain a description of the fluid–armature interaction that may be modeled, we will assume that the modes are well separated and that each mode may be described by a linear simple harmonic oscillator. The first four modes of the sensor are shown in Fig. 2. These diagrams were reproduced from analysis that was carried out at Schlumberger Research using the finite element package ANSYS. The mode of interest for the MEMS device considered in this study is the 3rd, in which the plate oscillates in a plane, thereby reducing the dimensionality of the problem.

3.1. Strain on the Plate

Once the plate is in motion, strain will be produced in any two connecting parts of the viscometer. The most important of these are the legs

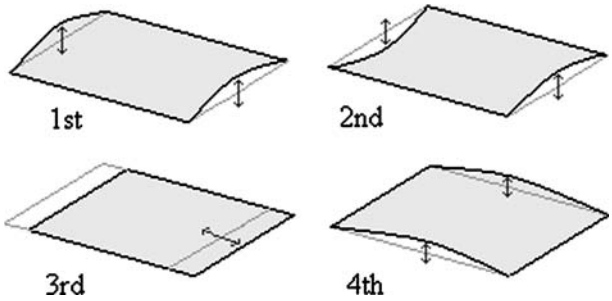

Fig. 2. Various modes of oscillation of the "spider".

that connect the plate to the main viscometer body. For simplicity, it is assumed that the oscillatory motion will result only in the deformation of these legs. The elastic restoring force for each individual leg is

$$F_{\mathrm{er}} \equiv \frac{s^3 E d A}{l^3}, \tag{4}$$

where s is the leg width, l is the length of the leg, d is the depth of the leg (also the plate depth), E is the Young's modulus of the leg material, and A is the amplitude of motion. Assuming that it is only dependent on the mass of the plate M_{p} $(=aBd\rho_{\mathrm{s}})$, we can write the undamped frequency for N legs as

$$\omega_0 = \sqrt{\frac{N F_{\mathrm{er}}}{A M_{\mathrm{p}}}} = \sqrt{\frac{N E s^3}{l^3 a B \rho_{\mathrm{s}}}} \tag{5}$$

where a is the length of the plate, B is the plate width, and ρ_{s} is the density of the plate material.

3.2. Forced Oscillations

3.2.1. Mechanics of the Infinite Plate

We assume that the plate oscillates in an infinite volume of liquid and is itself infinite in both the x and z directions. The plate is also assumed to lie in the x–z plane. The surface of the plate bounds an incompressible fluid. The plate is forced to oscillate in the x direction with simple harmonic motion confined to the x–z plane. The velocity of the plate, shown in Fig. 3, is thus $\mathbf{q} = [U_{\mathrm{p}}(t), 0, 0]^T$ with $U_p = U_0 Re(e^{-\imath\omega t})$, where ω is the frequency of oscillation and U_0 characterizes the amplitude of the motion.

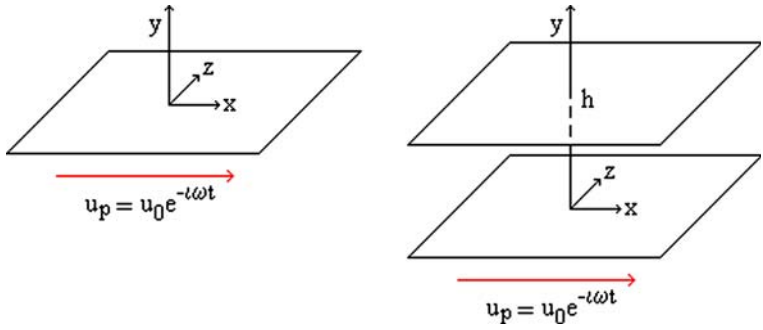

Fig. 3. Plane oscillating in the x-direction and in the vicinity of stationary top plate.

3.2.2. Newtonian Viscous Flow

We assume that the fluid moves according to a plane parallel shear flow [7] with velocity $\mathbf{q} = (u(y,t), 0, 0)^T$. With no applied pressure gradient, the Navier–Stokes equations (in the absence of gravity) therefore reduce to the one-dimensional diffusion equation,

$$\frac{\partial u}{\partial t} = \nu \frac{\partial^2 u}{\partial y^2}. \tag{6}$$

Equation (6) must be solved subject to appropriate boundary conditions. With no slip at the plate, we therefore impose

$$u(0,t) = U_p(t) = U_0 Re(e^{-\iota\omega t}), \tag{7}$$

$$u \to 0 \qquad \text{as} \qquad y \to \infty. \tag{8}$$

The solution is given by $u = U_0 e^{-\frac{y}{\delta}} Re(e^{\iota(\frac{y}{\delta} - \omega t)})$, where $\delta = \sqrt{\frac{2\nu}{\omega}}$ is the viscous penetration depth. Taking real parts, we find that

$$u = U_0 e^{-\frac{y}{\delta}} \cos\left(\frac{y}{\delta} - \omega t\right). \tag{9}$$

Another way of operating the device is to add a second (stationary) plate in the x–z plane above the oscillating plate. When such a plate is present at a height $y = +h$, the boundary conditions become

$$u(0,t) = U_0 Re(e^{-\iota\omega t}) \qquad \text{and} \qquad u(h,t) = 0. \tag{10}$$

We now find that

$$u = U_0 e^{-\frac{y}{\delta}} Re\left[e^{\iota(\frac{y}{\delta} - \omega t)} \left(\frac{1 - e^{-\frac{2}{\delta}(h-y)} e^{\frac{2}{\delta}\iota(h-y)}}{1 - e^{-\frac{2h}{\delta}} e^{\frac{2h}{\delta}\iota}} \right) \right] \tag{11}$$

and hence

$$u = U_0 e^{-\frac{y}{\delta}} \times$$
$$\left[\frac{\cos(\frac{y}{\delta} - \omega t) - e^{-\frac{2h}{\delta}} \cos(\frac{y-2h}{\delta} - \omega t) - e^{-\frac{2}{\delta}(h-y)} \cos(\frac{2h-y}{\delta} - \omega t) + e^{-\frac{2}{\delta}(2h-y)} \cos(-\frac{y}{\delta} - \omega t)}{1 - 2e^{-\frac{2h}{\delta}} \cos(2h/\delta) + e^{-\frac{4h}{\delta}}} \right]. \tag{12}$$

Presently Eqs. (9) and (12) will be used to determine the properties of the fluid.

3.2.3. Viscoelastic Flow

The simple model developed above may also be used to analyze the viscosity of non-Newtonian, and in particular viscoelastic fluids. We assume that a viscoelastic downhole fluid obeys the Maxwell equations of motion

$$\mathbf{q}_t + (\mathbf{q} \cdot \nabla)\mathbf{q} = -\frac{1}{\rho} \nabla p + \nabla \cdot \sigma \tag{13}$$

$$\nabla \cdot \mathbf{q} = 0 \tag{14}$$

where the stress tensor σ_{ij} is given by

$$\sigma_{\iota J t} + (\mathbf{q} \cdot \nabla)\sigma_{\iota J} - \frac{\partial q_\iota}{\partial x_k}\sigma_{kJ} - \frac{\partial q_J}{\partial x_k}\sigma_{k\iota} + \frac{1}{\theta}\sigma_{\iota J} = \frac{\nu}{\theta}\left(\frac{\partial q_\iota}{\partial x_J} + \frac{\partial q_J}{\partial x_\iota}\right). \tag{15}$$

Here $\theta = \frac{\nu}{G}$, where G is the shear modulus of the fluid. Since $\mathbf{q}$ is independent of x, the equations reduce to

$$\frac{\partial^2 u}{\partial t^2} + \frac{1}{\theta}\frac{\partial u}{\partial t} = \frac{\nu}{\theta}\frac{\partial^2 u}{\partial y^2}. \tag{16}$$

In a similar way to the Newtonian case, with no stationary plate present, Eqs. (7) and (8) are the appropriate boundary conditions. Equation (16) may be solved to yield

$$u = U_0 e^{-\sqrt{\frac{\omega}{\nu}}(1+\omega^2\theta^2)^{\frac{1}{4}} y \sin(\frac{\gamma}{2})} Re(e^{\iota(\sqrt{\frac{\omega}{\nu}}(1+\omega^2\theta^2)^{\frac{1}{4}} y \cos(\frac{\gamma}{2}) - \omega t)}), \tag{17}$$

where $\gamma = \arctan\frac{1}{\omega\theta}$. Taking real parts, we find that

$$u = U_0 e^{-\sqrt{\frac{\omega}{\nu}}(1+\omega^2\theta^2)^{\frac{1}{4}} y \sin(\frac{\gamma}{2})} \cos\left(\sqrt{\frac{\omega}{\nu}}(1+\omega^2\theta^2)^{\frac{1}{4}} y \cos(\gamma/2) - \omega t\right). \tag{18}$$

Once again, a second stationary infinite plate may be added in the x–z plane at $y = +h$, in which case the boundary conditions are given by Eq. (10). We then find that

$$u = U_0 Re\left[\left(\frac{\sinh(\lambda(h-y))}{\sinh \lambda h}\right) e^{-\iota\omega t}\right] \tag{19}$$

where

$$\lambda = \sqrt{\frac{\omega}{\nu}}(1+\theta^2\omega^2)^{1/4} e^{\iota\gamma/2}. \tag{20}$$

3.2.4. Frictional Force and Power on the Plate for Newtonian Flow

We may now use Eqs. (9), (12), (18) and (19) to analyze the properties of the fluid surrounding the plate. The frictional force S acts in the x-direction since this is the only direction in which the oscillating plate has a non-zero velocity component. S may be determined using the stress tensor σ_{ij} [8], and acts over a surface area of twice the product of the length and breadth of the plate. For Newtonian flow,

$$S = 2aB[\sigma_{yx}]_{y=0} = 2aB\left[\mu\frac{\partial u}{\partial y}\right]_{y=0}. \tag{21}$$

The power required to move the plate is defined by the product of the frictional force and the fluid velocity evaluated at the plate surface. For a viscometer in forced mode, the average power over a period of oscillation is

$$P\,|_{y=0} = \frac{\omega}{2\pi}\left|\int_0^{\frac{2\pi}{\omega}} Re(Su\,|_{y=0})\,dt\right|. \tag{22}$$

For the Newtonian case the fluid velocity, u, is given by Eq. (9). Using this in Eq. (21), and assuming that U_0 is real, we find that

$$S = -2aB\sqrt{(\omega\mu\rho)}U_0\cos\left(\omega t + \frac{1}{4}\pi\right). \tag{23}$$

The velocity of the oscillating plate is $U_p = U_0\cos\omega t$; we therefore observe a phase difference between this velocity and the frictional force. The relevant substitutions may now be made into Eq. (22) to give

$$|P|_{y=0}| = \frac{\omega}{2\pi}\left|\int_0^{\frac{2\pi}{\omega}} (-2aBU_0\cos(\omega t)\sqrt{(\omega\mu\rho)}U_0\cos(\omega t+\frac{\pi}{4}))dt\right|$$
$$= \frac{1}{\sqrt{2}}aBU_0{}^2\sqrt{\omega\mu\rho}. \tag{24}$$

Equation (24) may now be rearranged to yield

$$\mu = \frac{2}{\omega\rho}\left[\frac{|P|_{y=0}|}{aBU_0{}^2}\right]^2, \tag{25}$$

giving the viscosity as a function of the density, the power and U_0. With an added stationary plate at $y = h$, a similar calculation to that shown above may be performed. The average power in this case is given by

$$|P|_{y=0}| = \frac{U_0^2 aB\mu}{\delta}\left[\frac{e^{4h/\delta}+2e^{2h/\delta}\sin(2h/\delta)-1}{e^{4h/\delta}-2e^{2h/\delta}\cos(2h/\delta)+1}\right]. \tag{26}$$

In contrast to the case where no top plate is present, Eq. (26) cannot now be rearranged to give a simple explicit formula for the viscosity μ as the viscous penetration depth $\delta = \sqrt{2\mu/\rho\omega}$ appears in Eq. (26) in a complicated fashion. Notwithstanding this, Eq. (26) may be regarded as a transcendental equation for μ that could easily be solved.

In principle, therefore, Eqs. (25) and (26) allow the determination of the fluid viscosity provided U_0, ω, the power, the fluid density, and the dimensions of the plate are all known. The practical feasibility of using the viscometer in this mode will be discussed further in Section 4.

3.2.5. Viscoelastic Flow

Though in principle the calculations for the frictional force and the power on the plate may be carried out in the same way for a viscoelastic fluid as for a Newtonian fluid, matters are complicated by the fact that, though u is known (from Eq. (18) and Eq. (19), respectively) when the device is operated both without and with a stationary upper plate, the shear stress on the plate is no longer given by the simple formula $\mu u_y|_{y=0}$. Instead, it is necessary to solve the equation

$$\frac{\partial\sigma_{12}}{\partial t}+\frac{1}{\theta}\sigma_{12} = \frac{\nu}{\theta}u_y. \tag{27}$$

Though we omit the details for brevity, it is nevertheless possible to derive a (rather complicated) expression for the power on the plate. Once again, it is not possible to solve for the viscosity and write a closed-form expression for μ: however, the resulting equation could easily be solved (as for

the Newtonian case above when a top plate was added) to determine the viscosity as a function of the other measured parameters. We comment further on the viscoelastic case in Section 4.

3.3. Decaying Oscillations

We now consider the viscometer in what may be termed "plucked" mode. The plate will now resemble a damped harmonic oscillator with a corresponding decay rate. By analyzing the decay in oscillation amplitude we then aim to infer the viscosity and/or density of the surrounding fluid. Since we may need to ignore early oscillations which could exhibit irregular transient behavior, our aim is to identify conditions where the plate oscillates a relatively large number of times in the fluid before the oscillations decay completely. In this manner, a suitably large amount of data can be collected.

To operate the viscometer in "plucked" mode, the plate is moved to an arbitrary displacement (X) and held there by an external force. Measurements begin when the external force is removed and the plate is released with zero initial velocity. It is assumed that the legs around the edge of the plate provide some damping, and in addition the plate is retarded by the fluid shear stress ($\mu u_y|_{y=0}$) that acts over the top and bottom surface areas of the plate (of total area $2Ba$). For Newtonian flow, $u(y,t)$ is determined from Eq. (6), and the displacement $x(t)$ of the plate is described by

$$\rho_s d Ba \frac{d^2x}{dt^2} + r\frac{dx}{dt} + k^2 x = 2Ba(\mu u_y|_{y=0}). \tag{28}$$

Here, r characterizes the damping of the plate legs and k is the associated spring constant. Equation (6) must be solved subject to the boundary conditions

$$u(t) = \tfrac{dx}{dt} \qquad \text{at} \qquad y = 0 \tag{29}$$

$$u \to 0 \text{ as } y \to \infty \tag{30}$$

and the initial condition

$$u = 0 \qquad \text{at} \qquad t = 0. \tag{31}$$

We take a Laplace transform in t to recast the equation for $u(y,t)$ as an ordinary differential equation for $\hat{u}(y,s)$. The problem becomes

$$s\hat{u} - v\hat{u}_{yy} = 0, \tag{32}$$

$$\hat{u}(0,s) = s\hat{x} - x(0) \tag{33}$$

and

$$\hat{u}(\infty,s) = 0. \tag{34}$$

Since $y\sqrt{\frac{s}{\nu}} \to \infty$ as $Re(s) \to \infty$, we have

$$\hat{u}(y,s) = (s\hat{x} - x(0))e^{-y\sqrt{\frac{s}{\nu}}}. \tag{35}$$

We now take the Laplace transform of Eq. (28) to yield

$$(s^2 + \mathsf{A}s + \mathsf{B})\hat{x} - (s + \mathsf{A})x(0) = \mathsf{C}\mu\hat{u}_y|_{y=0}, \tag{36}$$

where $\mathsf{A} = \frac{r}{\rho_s Bda}$, $\mathsf{B} = \frac{k^2}{\rho_s Bda}$, and $\mathsf{C} = \frac{2}{\rho_s d}$. Equation (35) may now be differentiated with respect to y and evaluated at $y = 0$, before being substituted back into Eq. (36). An inverse Laplace transform may now be taken to yield

$$x = x(0)L^{-1}[f(s)], \quad f(s) = \frac{s + \mathsf{A} + \mathsf{C}\sqrt{\mu\rho s}}{s^2 + \mathsf{A}s + \mathsf{B} + \mathsf{C}\sqrt{\mu\rho}s^{\frac{3}{2}}}. \tag{37}$$

The Laplace inversion in Eq. (37) is complicated by the numerous singularities in $f(s)$. By multiplying $f(s)$ with its algebraic conjugate, $f(s)$ can be rewritten to show the singularities more clearly in the form

$$f(s) = \frac{(s + \mathsf{A})(s^2 + \mathsf{A}s + \mathsf{B}) - \mathsf{E}^2 s^2}{(s^2 + \mathsf{A}s + \mathsf{B})^2 - \mathsf{E}^2 s^3} + \frac{\mathsf{E}\mathsf{B}\sqrt{s}}{(s^2 + \mathsf{A}s + \mathsf{B})^2 - \mathsf{E}^2 s^3}, \tag{38}$$

where $\mathsf{E} = \mathsf{C}\sqrt{\mu\rho}$. We observe that four poles (with associated residues) will occur due to the quartic polynomial in the denominator of the two fractions. It can be assumed that the poles will be two pairs of complex conjugates that must have negative real parts for oscillation decay to occur. The poles are determined by finding the four roots of the quartic polynomial equation:

$$s^4 + (2\mathsf{A} - \mathsf{E}^2)s^3 + (2\mathsf{B} + \mathsf{A}^2)s^2 + 2\mathsf{B}\mathsf{A}s + \mathsf{B}^2 = 0. \tag{39}$$

A branch cut is introduced by the square root in the second term of Eq. (38). The inverse Laplace transform will have three main contributing terms, namely an exponential term for each complex conjugate pair and an algebraic term arising from the branch cut. We now approximate the solution by considering the behavior at different times.

3.3.1. Small Time Approximation

Though closed-form inversion of the Laplace transform in Eq. (37) is awkward, we may investigate the behavior of the viscometer for both small and large times. To do this we consider the asymptotic expansions of $f(s)$ for small time (large s) or large time (small s) (see [9]). For the small time behavior we expand $f(s)$ about $s=\infty$ to give

$$\begin{aligned} f(s) &= \frac{(s+\mathsf{A}+\mathsf{E}\sqrt{s})}{s^2}\left[1+\frac{\mathsf{E}}{\sqrt{s}}+\frac{\mathsf{A}}{s}++\frac{\mathsf{B}}{s^2}\right]^{-1} \\ &= \frac{1}{s}-\frac{\mathsf{B}}{s^3}+\frac{\mathsf{BE}}{s^{\frac{7}{2}}}+\mathsf{B}\frac{\mathsf{A}-\mathsf{E}^2}{s^4}+\frac{\mathsf{B}(\mathsf{E}^3-2\mathsf{EA})}{s^{\frac{9}{2}}}\cdots . \end{aligned} \tag{40}$$

We are now able to take the inverse Laplace transform to show that, when $t\sim 0$,

$$x(t)=x(0)\left[1-\frac{\mathsf{B}}{2}t^2+\frac{8\mathsf{BE}}{15\sqrt{\pi}}t^{\frac{5}{2}}+\mathsf{B}\frac{\mathsf{A}-\mathsf{E}^2}{6}t^3\right]+O(t^{7/2}). \tag{41}$$

The most important physical conclusion from Eq. (41) is that the first two terms (and hence the leading-order small time behavior) involve only the physical parameter B, implying that, soon after the viscometer is set into motion, its behavior depends only on the properties of the plate and not on the surrounding fluid.

3.3.2. Large Time Approximation

To determine the large time behavior, we expand $f(s)$ about $s=0$ to give

$$\begin{aligned} f(s) &= \frac{(\mathsf{A}+\mathsf{E}\sqrt{s}+s)}{\mathsf{B}}\left[1+\left(\frac{\mathsf{A}}{\mathsf{B}}s+\frac{\mathsf{E}}{\mathsf{B}}s^{\frac{3}{2}}+\frac{1}{\mathsf{B}}s^2\right)\right]^{-1} \\ &= \frac{\mathsf{A}}{\mathsf{B}}+\frac{\mathsf{E}}{\mathsf{B}}\sqrt{s}+\frac{\mathsf{B}-\mathsf{A}^2}{\mathsf{B}^2}s-\frac{2\mathsf{AE}}{\mathsf{B}^2}s^{\frac{3}{2}}+\frac{\mathsf{A}^3-2\mathsf{AB}-\mathsf{E}^2\mathsf{B}}{\mathsf{B}^3}s^2+\frac{3\mathsf{A}^2\mathsf{E}-2\mathsf{EB}}{\mathsf{B}^3}s^{\frac{5}{2}}+\cdots . \end{aligned}$$

Taking the inverse Laplace transform now gives

$$x(t)=x(0)\left[\frac{\mathsf{E}}{\mathsf{B}}\frac{\sqrt{\pi}}{t^{\frac{3}{2}}}-\frac{\mathsf{AE}}{\mathsf{B}^2}\frac{\sqrt{\pi}}{t^{\frac{5}{2}}}+\frac{(3\mathsf{A}^2\mathsf{E}-2\mathsf{EB})}{\mathsf{B}^3}\frac{3\sqrt{\pi}}{4t^{\frac{7}{2}}}\right] \quad (t\sim\infty). \tag{42}$$

The significance of this result lies in the fact that the analysis shows that, contrary to what might be anticipated, the ultimate decay of the oscillations is algebraic, rather than exponential. Since the analysis of many similar devices is based upon determining fitted exponential decay rates, the algebraic nature of the decay should be taken into account when interpreting real results from the viscometer.

3.3.3. Decaying Oscillations: Numerical Solution

Though technically a complete analysis of the viscometer operated in plucked mode only requires the solution of the Laplace inversion problem Eq. (37), a complete inversion is awkward and involved. A simpler way to proceed is to recast the problem and proceed numerically. For simplicity, we treat only the Newtonian case where a top plate is not present. Solving the fluid problem subject to the conditions $u(y,0)=0$, $x=x(0)$ at $t=0$, $u(0,t)=\dot{x}(t)$ and $u\to 0$ as $y\to\infty$ using a Laplace transform, we find that Eq. (28) may be rewritten as

$$\frac{d^2x}{dt^2}+\mathsf{A}\frac{dx}{dt}+\mathsf{B}x=-\frac{\mathsf{E}}{\sqrt{\pi}}\int_0^t\frac{\frac{d^2x(s)}{ds^2}}{\sqrt{t-s}}ds, \tag{43}$$

where $x=x(0)=X$ and $dx/dt=0$ at $t=0$. We now non-dimensionalize the problem in order to simplify the equation and identify the key parameter combinations. We let $x=X\tilde{x}$ and scale time using $t=\frac{\sqrt{W}}{k}\tilde{t}$ where $W=\rho_s Bda$ is the weight of the plate. If we further set $s=\frac{\sqrt{W}}{k}\tilde{s}$, then Eq. (43) becomes

$$\frac{d^2\tilde{x}}{d\tilde{t}^2}+\alpha\frac{d\tilde{x}}{d\tilde{t}}+\tilde{x}=-\beta\int_0^{\tilde{t}}\frac{\frac{d^2\tilde{x}(\tilde{s})}{d\tilde{s}^2}}{\sqrt{(\tilde{t}-\tilde{s})}}d\tilde{s}, \tag{44}$$

where $\alpha=\frac{r}{k\sqrt{W}}$ and $\beta=\frac{2\sqrt{\mu\rho}Ba}{\sqrt{\pi k}W^{\frac{3}{4}}}$ are dimensionless variables whose values are determined by the material properties of the plate, and the viscosity and the density of the surrounding fluid. Equation (44) may now be solved numerically.

We define $\tilde{x}_i$ to be the value of $\tilde{x}(\tilde{t})$ at time $\tilde{t}=\tilde{t}_i$ with $i=0.\ldots.n$ and $t_0=0$. We employ a constant time step $\Delta\tilde{t}$ so that $\tilde{t}_{i+1}-\tilde{t}_i=\Delta\tilde{t}$. The initial conditions are that the plate starts from a stationary position (with zero velocity) at a distance X from the origin. Thence

$$\frac{d\tilde{x}(0)}{d\tilde{t}}=0 \qquad \text{and} \qquad \tilde{x}(0)=1. \tag{45}$$

We approximate the first and second derivatives of $\tilde{x}$ with respect to $\tilde{t}$ using central differences [10] so that

$$\frac{d\tilde{x}}{d\tilde{t}}=\tilde{x}'(i)\simeq\frac{\tilde{x}_{i+1}-\tilde{x}_{i-1}}{2\Delta\tilde{t}} \tag{46}$$

and

$$\frac{d^2\tilde{x}}{d\tilde{t}^2}\Rightarrow\tilde{x}''(i)=\frac{\tilde{x}_{i+1}-2\tilde{x}_i+\tilde{x}_{i-1}}{(\Delta\tilde{t})^2}. \tag{47}$$

To deal with the integral term in Eq. (43), we assume that $\tilde{x}''$ is constant on the interval $[\tilde{t}_j, \tilde{t}_{j+1}]$ and use the trapezium rule. Thus, for $i = 1, 2, \ldots$.

$$-\beta \int_0^{\tilde{t}_i} \frac{\tilde{x}''(\tilde{s})}{\sqrt{\tilde{t}-\tilde{s}}} d\tilde{s} \simeq -\beta \sum_{j=1}^{i} \int_{(j-1)\Delta\tilde{t}}^{j\Delta\tilde{t}} \frac{\tilde{x}''(j)+\tilde{x}''(j-1)}{2\sqrt{i\,\Delta\tilde{t}-\tilde{s}}} d\tilde{s}$$
$$= -\beta \sum_{j=1}^{i} (\tilde{x}''(j)+\tilde{x}''(j-1))\sqrt{\Delta\tilde{t}}(\sqrt{i-j+1}-\sqrt{i-j}).$$

This allows Eq. (43) to be approximated by

$$\frac{\tilde{x}_{i+1}-2\tilde{x}_i+\tilde{x}_{i-1}}{(\Delta\tilde{t})^2} + \alpha\left(\frac{\tilde{x}_{i+1}-\tilde{x}_{i-1}}{2\Delta\tilde{t}}\right) + \tilde{x}_i + \beta\left(\frac{\tilde{x}_{i+1}-\tilde{x}_i-\tilde{x}_{i-1}+\tilde{x}_{i-2}}{(\Delta\tilde{t})^{\frac{3}{2}}}\right)$$
$$= -\beta \sum_{j=1}^{i-1} \frac{\tilde{x}_{j+1}-\tilde{x}_j-\tilde{x}_{j-1}+\tilde{x}_{j-2}}{(\Delta\tilde{t})^{\frac{3}{2}}}(\sqrt{i-j+1}-\sqrt{i-j}). \tag{48}$$

This can be rearranged to give $\tilde{x}_{i+1}$ in terms of $\tilde{x}_i$, $\tilde{x}_{i-1}$, and $\tilde{x}_{i-2}$ so that all the $\tilde{x}_i$ may be determined for $i \geqslant 3$. To allow the calculation to begin, we need to determine $\tilde{x}_0$, $\tilde{x}_1$, and $\tilde{x}_2$ independently. Since $\tilde{x}_0 = 1$ and $\tilde{x}'(0) = 0$, a forward difference may be used to show that $\tilde{x}_0 = \tilde{x}_1 = 1$. Since the integral term in Eq. (44) is zero when $\tilde{t} = 0$, the scheme given by Eq. (48) may now be applied with $i = 1$ and the right-hand side set to zero to yield the value of $\tilde{x}_2$ and thus allow the calculation to begin. For simplicity, in this study we ignore the damping of the legs and set $r = 0$, so that $\alpha = 0$. The final (dimensionless) numerical scheme to determine the $\tilde{x}_i$ is thus

$$\begin{aligned}
\tilde{x}_0 &= 1 \\
\tilde{x}_1 &= 1 \\
\tilde{x}_2 &= 1 - \frac{2(\Delta\tilde{t})^2}{2+2\beta\sqrt{\Delta\tilde{t}}} \\
\tilde{x}_{i+1} &= \left(\frac{2(\Delta\tilde{t})^2}{2+2\beta\sqrt{\Delta\tilde{t}}}\right)\left[\tilde{x}_i\left(\frac{2}{(\Delta\tilde{t})^2}-1+\frac{\beta}{(\Delta\tilde{t})^{\frac{3}{2}}}\right)\right. \\
&\quad +\tilde{x}_{i-1}\left(\frac{\beta}{(\Delta\tilde{t})^{\frac{3}{2}}}-\frac{1}{(\Delta\tilde{t})^2}\right) - \tilde{x}_{i-2}\left(\frac{\beta}{(\Delta\tilde{t})^{\frac{3}{2}}}\right) \\
&\quad \left. -\beta \sum_{j=1}^{i-1} \frac{\tilde{x}_{j+1}-\tilde{x}_j-\tilde{x}_{j-1}+\tilde{x}_{j-2}}{(\Delta\tilde{t})^{\frac{3}{2}}}(\sqrt{i-j+1}-\sqrt{i-j})\right].
\end{aligned} \tag{49}$$

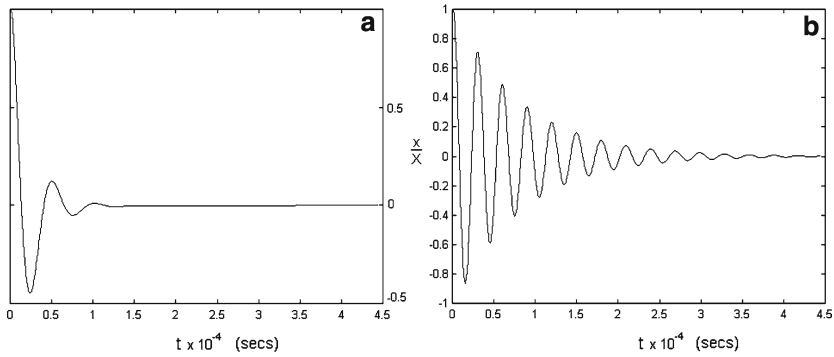

Fig. 4. (a) Numerical solution for $\beta = 1$; (b) numerical solution for $\beta = 0.1$. (Vertical axis: dimensionless displacement x/X. Horizontal axis: time (units of 10^{-4} s)).

The key dimensionless quantity in this system is β; its magnitude will determine the range and suitability of the viscometer. Numerical plots of the solution with $\mu = 0$ may be used with Eq. (5) to find the vacuum frequency of the plate and infer the constant k. We find that $k^2 = 9025\,\mathrm{kg{\cdot}s^{-2}}$. The full numerical solution of the problem now allows us to estimate what sorts of fluids the current viscometer specification may be suitable for. Typical illustrative numerical solutions are shown in Fig. (4) (plots produced in MATLAB [11]) . When $\beta = 1$ we observe that the system is overdamped and will provide too few oscillations to allow helpful measurements to be made. When $\beta = 0.1$ however (plot (b) of Fig. (4)), the number of oscillations and decay produced is clearly much more suitable for data collection. In general, numerical experiments show that the ideal value for β lies between about 0.001 and 0.1. With $\rho_s = 2320\,\mathrm{kg{\cdot}m^{-3}}$, $a = 2.4\,\mathrm{mm}$, $B = 1.6\,\mathrm{mm}$, and $d = 20\mu\mathrm{m}$ we find that $W = 0.178 \times 10^{-6}\,\mathrm{kg}$ and $\beta = \Lambda\sqrt{\mu\rho}$ where $\Lambda \sim 0.051\,\mathrm{kg^{-1}{\cdot}\ m^2{\cdot}s^{1/2}}$. We conclude that the current MEMS viscometer specification is suitable for fluids that satisfy $3.845 \times 10^{-4}\,\mathrm{kg^2{\cdot}m^{-4}{\cdot}s^{-1}} < \mu\rho < 3.845\,\mathrm{kg^2{\cdot}m^{-4}{\cdot}s^{-1}}$. At the low end of this range the fluid would be similar to argon at a temperature of 293 K and a pressure of 1 MPa (where the density is about $16\,\mathrm{kg{\cdot}m^{-3}}$ and the viscosity about $2.2\,\mu\mathrm{Pa{\cdot}s}$) while the high end of the range corresponds to methylbenzene at a temperature of 293 K and a pressure of 99 MPa (where the density is about $922\,\mathrm{kg{\cdot}m^{-3}}$ and the viscosity about $4\,\mathrm{mPa{\cdot}s}$).

4. CONCLUSIONS

We have analyzed a new type of MEMS viscometer in both "forced" and "plucked" modes. In forced mode, we were able to derive either

closed-form expressions or equations for the viscosity as a function of the density, power, amplitude and physical properties of the plate. Though in principle this provides a very easy method of determining the viscosity of drilling fluids, it requires knowledge of both U_0 and the power of the plate, both of which may be hard to measure in practice. Indeed, it may not even be easy to be sure of some of the physical dimensions and properties of the plate and in particular the legs. The robustness of the system when operated in forced mode is also a matter that must be considered. It is possible that continued operation may prove too much for the integrity of the legs, and consequently the life of the device may be short. Clearly a sustained experimental program is required. If the device could be made to function in forced mode however, it is clear from the work carried out above that it could be used to measure both Newtonian and non-Newtonian fluid properties.

In plucked mode, the device has been analyzed to the extent that we have been able to predict the type of fluid that it will be suitable for. Evidently more experimental work is required, but this feasibility study seems to show that the device could work well in this mode of operation. Though the details of the scheme given by Eq. (49) would change, the analysis carried out above could also be used to analyze the performance of the viscometer for non-Newtonian fluids and for versions of the device that included a top plate.

ACKNOWLEDGMENTS

The authors acknowledge Eric Donzier and Olivier Vancauwenberghe, of Schlumberger-Doll Research, for their efforts with the MEMS design, Fredrick Marty and Bruno Mercier of ESIEE for MEMS fabrication, and Maria Manrique de Lara, of Schlumberger Cambridge Research, for finite element calculations.

REFERENCES

1. R. Mostert, P. S. Van der Gulik, and H. R. Van den Berg, *Physica A* **156**:909 (1989).
2. H. Ockendon and J. R. Ockendon, *Viscous Flow* (Cambridge University Press, 1995), pp. 1–13.
3. A. Besq, C. Malfoy, A. Pantet, P. Monnet, and D. Righi, *Appl. Clay Sci.* **23**:275 (2003).
4. V. L. Spiering, S. Bouwstra, and R.M.E.J. Spiering, *Sensor Actuator* **A.39**:149 (1993).
5. K. E. Petersen, *Proc. IEEE* **70**:420 (1982).
6. A. R. H. Goodwin, E. P. Donzier, O. Vancauwenberghe, A. D. Fitt, K. A. Ronaldson, W. A. Wakeham, M. M. de Lara, F. Marty, and B. Mercier, *J. Chem. Eng. Data* **51**:190 (2006).
7. D. J. Acheson, *Elementary Fluid Dynamics* (Clarendon Press, 1990), pp. 33–38.

8. L. D. Landau and E. M. Lifshitz, *Fluid Mechanics* (Pergamon Press, 1959), pp. 47–51, 94.
9. K. Ronaldson, *Mathematical Modelling of MEMS Viscometers and Densitometers* (Thesis submitted September 2005, University of Southampton, UK).
10. C.E. Gerald and G. Wheatley, *Applied Numerical Analysis* (Addison-Wesley, World Student Series, 1997), pp. 363–368.
11. A. Gilat, *MATLAB, An Introduction With Applications* (John Wiley, New York 2005), pp. 107–130.